

THE ATMOSPHERIC AEROSOLS AND THEIR EFFECTS ON CLOUD ALBEDO AND RADIATIVE FORCING

Sabina Stefan¹, Gabriela Iorga², Maria Zoran³

¹University of Bucharest Faculty of Physics, P.O. Box MG-11, Bucharest, ROMANIA E-mail: sabina_stefan@yahoo.com

² University of Bucharest , Faculty of Chemistry, Department of Physics, Regina Elisabeta Avenue, No. 4-12 Bucharest, ROMANIA

³INOE 2000, Atomistilor Street No 1, Magurele, Bucharest, ROMANIA

The aim of this study is to provide results of the theoretical experiments in order to improve the estimates of indirect effect of aerosol on the cloud albedo and consequently on the radiative forcing. The cloud properties could be changed primarily because of changing of both the aerosol type and concentration in the atmosphere. Only a part of aerosol interacts effectively with water and will, in turn, determine the number concentration of cloud droplets (CDNC). We calculated the CDNC, droplet effective radius (r_{eff}), cloud optical thickness (τ), cloud albedo and radiative forcing, for various types of aerosol. Our results show into what extent the change of aerosol characteristics (number concentration and chemical composition) on a regional scale can modify the cloud reflectivity. Higher values for cloud albedo in the case of the continental (urban) clouds were obtained.

Keywords: aerosol, cloud albedo, radiative forcing

1- INTRODUCTION

Aerosols are present in both troposphere and stratosphere and mostly throughout the atmospheric boundary layer at number concentrations depending upon factors such as location, atmospheric conditions, annual and diurnal cycles and presence of local sources.

Aerosols have a direct radiative forcing because they scatter and absorb solar and infrared radiation in the atmosphere. Aerosols also alter warm, ice and mixed-phase cloud formation processes by increasing droplet number concentrations and ice particle concentrations and thereby cause an indirect radiative forcing associated with the changes in cloud microphysical and optical properties. Furthermore, aerosols that are highly absorbing of solar radiation, such as black carbon, may reduce cloud cover and liquid water content by heating the cloud and the environment within which the cloud forms. This is known as the semi-direct effect [10], because it is the result of direct interaction of aerosols with radiation but also influences climate indirectly by altering clouds. The net effect of aerosols on climate depends upon the summa of all three above mechanisms.

An important characteristic of aerosols is that they have short atmospheric lifetimes and therefore cannot be simply considered as a long-term offset to the warming influence of greenhouse gases; aerosols also show a large variability in their physical, chemical and optical properties. Among other factors, such as detailed and accurate emission inventories of the aerosol components at global scale, the above characteristics make the quantification of radiative aerosol effects more difficult.

As in the last Assessment Report of IPCC [27] the strong impact of the aerosol particles on climate is emphasized, the scientific community agreed that investigation of the their

radiative effects is important to reduce the associated uncertainties in order to obtain better estimates and to gain knowledge in the framework of anthropogenic climate change due to aerosols.

The indirect radiative forcing of aerosols through their effect on liquid-water clouds consists of two parts: the 1st indirect effect (increase in droplet number associated with increases in aerosols) and the 2nd indirect effect (decrease in precipitation efficiency associated with increases in aerosols). The 1st indirect effect has strong observational support [28]. This includes studies that established a link between changes in aerosols, cloud droplet number and cloud albedo (optical depth).

The quantification of indirect radiative forcing by aerosols is especially difficult because, in addition to the variability in aerosol concentrations, other complicated processes (eg. gas-to-particles conversions, in-cloud aerosol processing) must be accurately considered. Cloud droplet nucleation involves aerosol particles that can be activated to CCN (cloud condensation nuclei) and according to, for example, Twomey [25], Pruppacher and Klett [20] and Penner et al [21], this process is strongly dependent on aerosol characteristics.

There are two general methods that have been used to relate changes in CDNC to changes in aerosol concentrations. The first and simplest approach uses an empirical relationship that directly connects some aerosol quantity to CDNC ([25], [15], [3]).

The second method that has been used to relate changes in CDNC to changes in aerosol concentrations is based on a prognostic parameterisation of the cloud droplet formation process ([8], [1, 2]). Most state of the art GCMs now have prognostic treatment of cloud water rather than a diagnostic treatment and this has led to significant progress in the representation of clouds globally. Prognostic treatment of liquid water tends to give a better prediction of cloud water path, and the way that it changes with diabatic heating, turbulence and so on.

The prognostic approach requires detailed information about the spectrum and chemical composition of the aerosol and parameterisation of the nucleation process and growth processes of the formed cloud condensation nuclei that will lead to cloud optical properties. Martin et al. [18] proposed a one-to-one correspondence between number concentration of cloud condensation nuclei (CCN) and the cloud droplet number concentration (CDNC) in the sub-cloud layer in clean maritime air-masses. We assumed this suggestion in Section 3 for calculations of the effective radius (r_{eff}) and cloud optical thickness (τ). The CDNC and r_{eff} were calculated for various types of aerosol using the parameterisations proposed by Abdul-Razzak [1,2] and Liu and Daum [17], respectively.

Several studies prove that, during the cloud-aerosol interaction, cloud geometrical thickness can change ([6], [12]), so the predicted CDNC may change combining the effects of changes in droplet concentrations and changes in geometrical thickness of clouds ([9]). The reported results show that liquid water path (LWP) either is constant ([4], [5], [15]), or does not remain constant with change in aerosol concentration ([9]). Moreover, the results reported by Han et al [9] from analysed satellite data show for most continental clouds with $\tau > 15$ clouds albedo increase with decreasing r_{eff} and for the $\tau < 15$ over oceans, cloud albedo decreases with decreasing r_{eff} .

Section 2 contains theoretical considerations about the aerosol data and parameterisations used, as well as the calculations of cloud droplet effective radius and of the cloud optical depth for each spectral interval considered. In Section 3, using the properties of clouds emphasized in Section 2, we calculated the cloud albedo as a function of CDNC in connection to the changes in liquid water content (LWC) and the cloud droplet effective radius (r_{eff}). This section also contains the results related to changes in shortwave radiative forcing as function of cloud albedo, optical thickness and liquid water path. Section 4 summarizes the results obtained.

2. AEROSOL DATA AND CALCULATED CLOUD OPTICAL PROPERTIES

2.1 Aerosol data

The atmospheric aerosols are a chemical mixture of multiphase, dispersed solid and/or liquid particles suspended in the ambient air. The size of aerosol particles ranges over more than four orders of magnitude from a few nm to around 100 μm . From a climatic point of view, probably the most important subset of atmospheric aerosols are those in the fine and accumulation mode, with size from 0.1 μm to a few micrometers. The highest aerosol concentrations are usually found in urban areas, reaching up to 10^8 and 10^9 particles per cc [23]. Aerosols that are comprised of water soluble compounds are efficient cloud condensation nuclei (CCN). Examples of water soluble aerosols are sulfate and nitrate containing aerosols and sea salt aerosol. In background (unpolluted) continental conditions, smaller particles are more likely to be water soluble; about 80% of the particles in the 0.1 to 0.3 μm size range is comprised of water soluble particles. Over oceans, however, much of the coarse particle mode, comprised of sea salt aerosols, are also water soluble. Water soluble aerosols are hygroscopic; they are capable of attracting water vapor from the air. The size of hygroscopic particles varies with relative humidity, leading to changes in optical properties as well. Measurements of chemical composition reported in literature show that the continental aerosol contains 15-30% sulfate, while marine aerosol contains somewhat more (30-60%), and clearly most of the sulfate for both types of aerosol can be found in the accumulation mode.

With respect to above considerations, the aerosol types used in this study were urban aerosol and marine aerosol with an aerosol size distribution given by the sum of three lognormal size distributions, as described by the equation 1:

$$\frac{dn_a}{d \log a} = \sum_{i=1}^3 \frac{n_{a,i}}{\sqrt{2\pi} \log \sigma_i} \exp\left(-\frac{[\log(a/a_{m,i})]^2}{2(\log \sigma_i)^2}\right) \quad (1)$$

where $n_{a,i}$, $a_{m,i}$ and σ_i are the total number concentration, geometric mean dry radius, and geometric standard deviation of aerosol mode i , respectively. The modes are: $i = 1$ nucleation mode, $i = 2$ accumulation mode and $i = 3$ coarse mode.

Table 1. Modal parameters of aerosol number size distributions

	$n_{r,i}$ (cm^{-3})	r_i (μm)	$\log \sigma_i$
M-HF	100	0.027	0.25
	120	0.105	0.11
	6	0.210	0.45
M-W	340	0.005	0.20
	60	0.035	0.30
	3.1	0.310	0.43
U-J	$9.93 \cdot 10^4$	0.006	0.245
	$1.11 \cdot 10^3$	0.007	0.666
	$3.64 \cdot 10^4$	0.025	0.337
U-W	$21.2 \cdot 10^3$	0.006	0.240
	$37 \cdot 10^3$	0.031	0.297
	4.9	0.540	0.328

The marine aerosols we considered here are that of Whitby [26], which consist of 61% of $(\text{NH}_4)_2\text{SO}_4$ and 39% NaCl, and that of Hoppel and Frick, [11] which are assumed to be pure ammonium sulfate. The chemical composition of the urban aerosols is assumed to be a

mixture of ammonium sulfate (50%), ammonium nitrate (30%) and an insoluble material (22%), [19]. Table 1 contains the modal parameters of the urban aerosols as given by Jaenicke (U-J), [14] and Whitby (U-W), [26] and marine aerosols of Whitby (M-W) and Hoppel and Frick (M-HF).

2.2. Activation of the aerosols

The parameterisation used to compute the fraction of activated aerosol particles as function of supersaturation S_m (Figure 1. and Figure 2.), for the aerosol mode “i” is that resulted from the analysis of Abdul-Razzak [1,2], pertaining to the cloud droplets formation from an activated aerosol in a parcel of air rising adiabatically.

$$f_i(S_m) = \frac{1}{2} \cdot \operatorname{erfc} \left\{ \frac{\ln \left[f_1(\ln \sigma) \cdot \left(\frac{\xi}{\eta} \right)^{3/2} + f_2(\ln \sigma) \cdot \left(\frac{S_m^2}{\eta + 3\xi} \right)^{3/4} \right]}{3\sqrt{2} \cdot \ln \sigma} \right\} \quad (2)$$

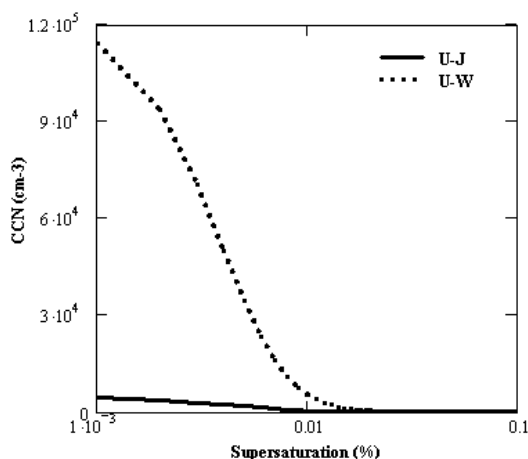


Figure 1. Number concentration of activated aerosol particles (in cm^{-3}) versus supersaturation as is described by equation 1 for urban aerosol.

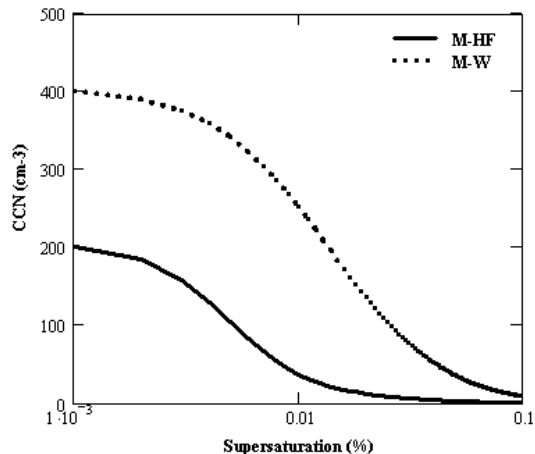


Figure 2. Number concentration of activated aerosol particles (in cm^{-3}) versus supersaturation as is described by equation 1 for marine aerosol.

where the two functions of standard deviation are considered as:

$$f_1(\ln \sigma) = 0.5 \cdot \exp\{2.5 \cdot (\ln \sigma)^2\}, \text{ and } f_2(\ln \sigma) = 1 + 0.25 \cdot \ln \sigma, \text{ respectively.}$$

One can observe the significant differences between the cloud condensation nuclei for aerosols in urban and marine air masses that might be explained in part by the differences in the aerosol number concentration and in part by the differences in the assumed chemical composition. For marine aerosol at a supersaturation of 0.5%, there is activated a number of order of 10^2 particles per cm^3 in both cases of chosen aerosol distribution. At the same supersaturation, the CCN concentration is of order of 10^3 for Whitby and of 10^4 for Jaenicke distribution.

2.3. Relationships between effective radius, liquid water path and the cloud optical depth.

Effective radius

The effective radius can be parameterised as a “1/3” power law of the ratio between the cloud liquid water content and the cloud droplet number concentration, with some pre-factors which are dependent of spectral dispersion of droplet size distribution ([18], [17]).

$$r_{eff} = PF \cdot \left(\frac{LWC}{N_{CDNC}} \right)^{\frac{1}{3}} \quad (3)$$

where the pre-factor PF has been computed as:

$$PF = 62.04 \cdot \frac{(1 + 2d^2)^{2/3}}{(1 + d^2)^{1/3}} \quad (4)$$

Here d signifies the spectral dispersion ($d = \frac{\sigma}{r}$) of droplet size distribution. An increase in d may act to negate the effect of increased N on r_{eff} and on cloud reflectivity [17]. We have assumed that the spectral dispersion of the aerosol number size distribution characterizes the CDNC size distributions and we have considered only the values of the spectral dispersion corresponding to the accumulation mode of the various aerosol types.

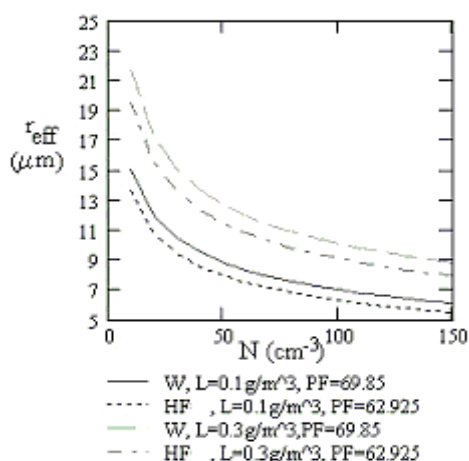


Figure 3. Cloud droplet effective radius as a function of CDNC for marine air masses.

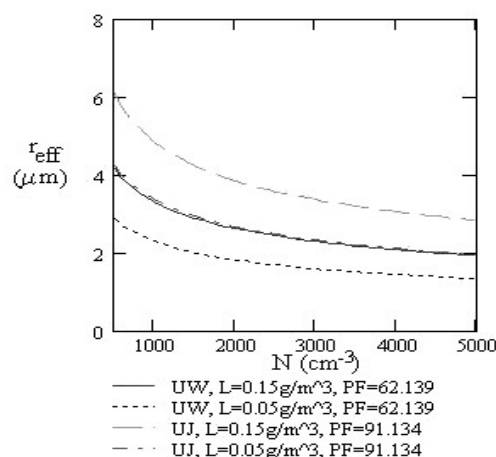


Figure 4. Cloud droplet effective radius as a function of CDNC for urban air masses.

In liquid water clouds, the effective radius, r_{eff} can be further used to express the cloud optical thickness, the single scattering albedo and the asymmetry factor.

Figures 3 and 4 show the effective radius dependence of CDNC for different two values of liquid water content, for urban and maritime stratiform clouds. The two values considered for liquid water content in case of urban clouds were 0.05 g/m^3 , as an extreme case, and 0.15 g/m^3 , and for maritime case are 0.1 g/m^3 and 0.3 g/m^3 , respectively [13].

Results show the strong dependences between the effective radius, liquid water content, and spectral dispersion. For the maritime case, results show, for the liquid water content of 0.1 g/m^3 , effective radius range is between 6 and $15 \mu\text{m}$ and between 9 and $20 \mu\text{m}$ for a liquid water content of 0.3 g/m^3 . An increase of liquid water content leads to higher values for effective radius, depending on the CDNC values. The values are similar with those measured by Han et al. [9]. The dependences are similar in the case of continental clouds; one can observe the smaller values of r_{eff} for higher concentrations of CDNC. The most likely values for effective radius for continental stratiform clouds lie in the range $2 \div 4 \mu\text{m}$. The values are

similar with those measured by Han et al. [9] and simulated by Boucher and Lohmann [3] with ECHAM and LMD GCM models.

Asymmetry factors

Starting from effective radius values, we have computed the asymmetry factors, g_1 and g_2 for visible and near-infrared ranges of the solar part of electromagnetic spectrum. [7]: the visible (0.25÷0.68 μm), and near infrared (0.68÷4.0 μm).

$$\begin{aligned} g_1(r_{\text{eff}}) &= 0.79 + 0.11 \cdot \log r_{\text{eff}} - 0.03 \cdot (\log r_{\text{eff}})^2 \\ g_2(r_{\text{eff}}) &= 0.79 + 0.04 \cdot \log r_{\text{eff}} + 0.19 \cdot (\log r_{\text{eff}})^2 - 0.08 \cdot (\log r_{\text{eff}})^3. \end{aligned} \quad (5)$$

as it is considered in the ECHAM GCM model, where the single scattering properties of clouds are derived from Mie theory.

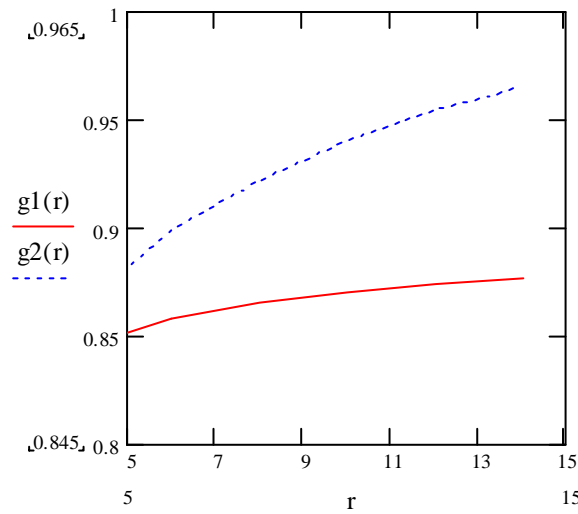


Figure 5. The dependence of g_1 and g_2 values as a function of effective radius

This parameterisation involves that at the higher values of the effective radius, there are the higher difference between values for visible and near infrared of the asymmetry parameter. For example for r_{eff} in the range 1÷2 μm , the differences between g_1 and g_2 values are too small and could be considered as negligible. In Fig. 5 it is shown the dependence of g_1 and g_2 values for effective radius between 5 and 15 μm .

Liquid water path and the cloud optical depth

Another important parameter for study of the albedo of clouds and consequently of the radiative forcing is liquid water path LWP (gm^{-2}), the product between the liquid water content (LWC) and the cloud geometrical thickness. The LWC (g/m^3), cloud droplet number concentration (cm^{-3}) and the effective radius (μm) are related by the following equation:

$$LWC = \frac{4}{3} \pi r_{\text{eff}}^3 \rho N \quad (6)$$

where ρ is the water density.

In order to investigate the dependence of optical depth τ on liquid water path LWP we have used the correlation between τ , effective radius r_{eff} and LWP:

$$\tau = \frac{3}{2} \cdot \frac{LWP}{\rho \cdot r_{\text{eff}}} \quad (7)$$

We have considered in further computations of cloud parameters the values of liquid water path below 150 g/m², tacking into account thus only non-precipitating stratiform clouds. In addition we have assumed all CCN become cloud droplets [18]. LWP increases with the third power of the effective radius.

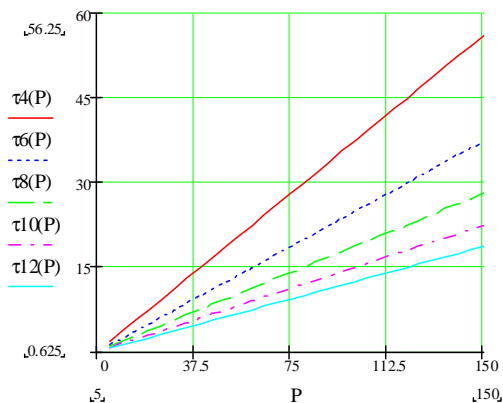


Figure 6. Optical thickness *versus* liquid water path for marine clouds and effective radius values of 4, 6, 8, 10 and 12 μm and cloud base at 100m.

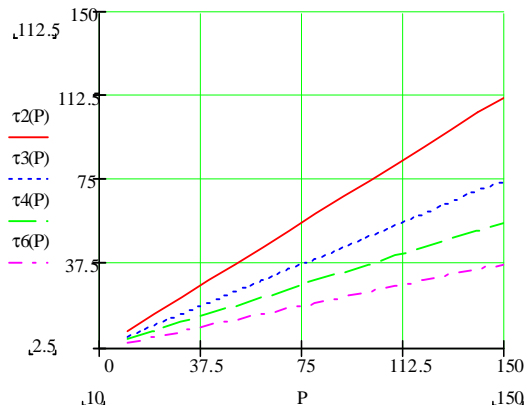


Figure 7. Optical thickness *versus* liquid water path for urban clouds and effective radius values 2, 3, 4 and 6 μm and cloud base at 500m.

Figures 6 and 7 show the dependence of τ of liquid water path (symbol P) in the case of marine and urban stratiform clouds with geometrical thickness of 100 m and 500 m, respectively. Regarding the dependence of τ of r_{eff} for a fixed value of LWP we have found an increase of optical thickness with the decrease of effective radius, so that for r_{eff} 12 μm and a value of LWP of 150 g/m², corresponds a value of about 18 in case of a cloud with geometrical thickness of 100 m. We also note the dependence of τ on the both geometrical thickness and the type of clouds.

3. CLOUD ALBEDO AND INDIRECT RADIATIVE FORCING

The cloud albedo, R_c , was computed taking into account the two-stream approximation of a nonabsorbing, horizontally homogeneous cloud [16]:

$$R_c = \frac{\sqrt{3}(1-g)\tau}{2 + \sqrt{3}(1-g)\tau} \quad (8)$$

where τ is the optical depth of the cloud, and g denotes the asymmetry factor.

Figure 8. presents the differences in cloud albedo values for marine clouds with an effective radius of 10 and of 8 μm for three fixed values of cloud geometrical thickness z of 100 m, 500m and 800m, for the spectral interval 0.25-0.68 μm. The differences in associated forcing values as a function of relative increase in CDNC are shown in Fig. 9.

We can observe the influence of the type of clouds so, the type of aerosols, in Figs. 10 and 11, that show differences larger in the both cloud albedo and indirect radiative forcing values for urban clouds, in the same conditions as marine clouds.

The computed albedo values for cloud effective radius of 4, 6, 8 and 10 μm in function of cloud droplet number concentration, for the spectral interval 0.68-4.0 μm show the dependence of the albedo on the both effective radius and cloud droplet number concentration: the albedo increase with the increase of CDNC and decrease when effective

radius increase. Therefore, in urban clouds where the droplets are smaller and CDNC larger, the albedo values are larger than in marine clouds [24].

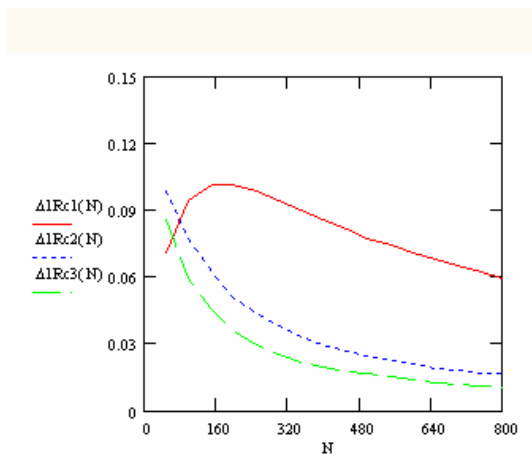


Figure 8. Differences between cloud albedo values computed for effective radius of 10 μ m and 8 μ m, respectively, in case of marine clouds, versus CDNC; spectral range 0.25-0.68 μ m and cloud geometrical thickness 100(c1), 500(c2), 800(c3) m.

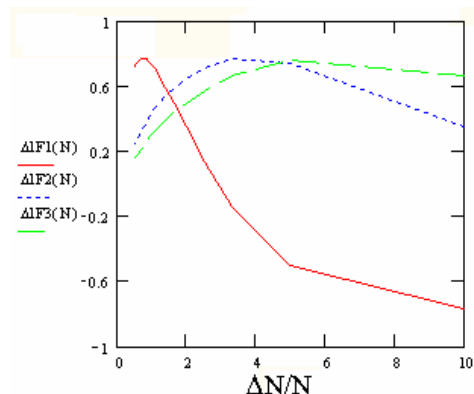


Figure 9. Differences between radiative forcing values in the same conditions as in Fig.8, but as function of relative increase in CDNC.

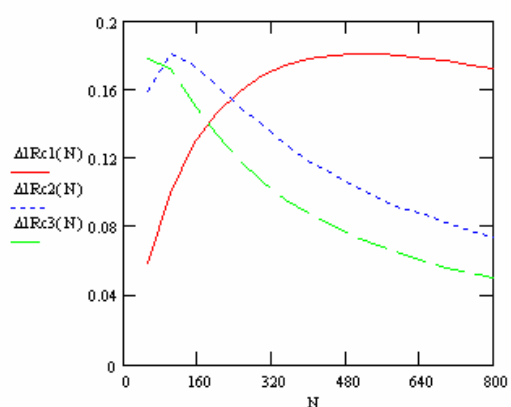


Figure 10. The same like in Fig.8 but for urban clouds

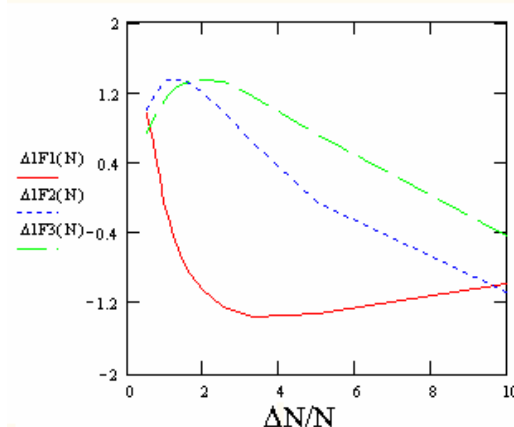


Figure 11. The same like in Fig.9 but for urban clouds

The indirect radiative forcing decrease faster when the effective radius of cloud increase, as in Fig.13.

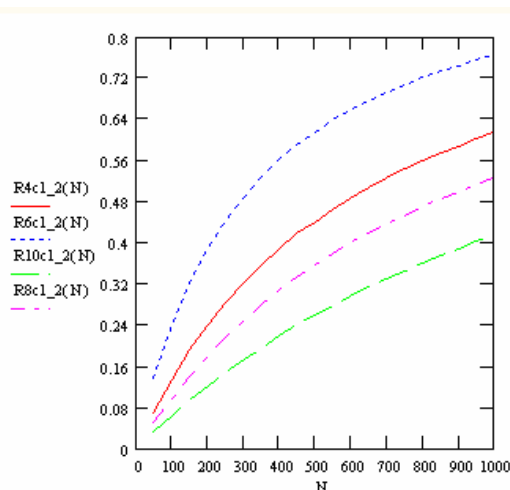


Figure 12. Albedo estimates for cloud effective radius of 4, 6, 8 and 10 μm in function of cloud droplet number concentration of marine cloud, for the spectral interval 0.68-4.0 μm .

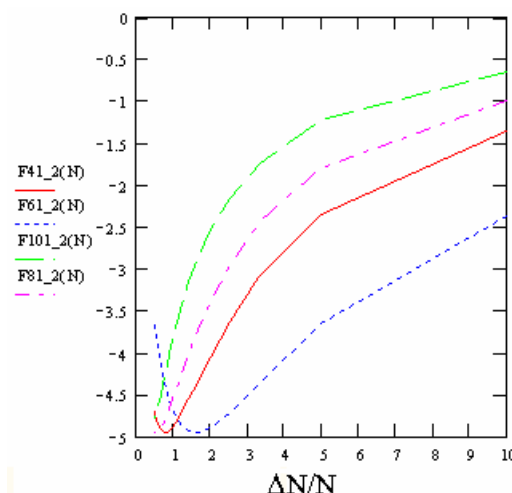


Figure 13. Dependence of radiative forcing of the relative increase in the cloud droplet number concentration for conditions in Fig. 12.

4. SUMMARY

Present work provide estimates for cloud albedo and associated indirect forcing for different aerosol types (marine and urban) as a function of increase in cloud droplet number concentration as result of increase in aerosol number concentration.

The different chemical composition of the aerosol types has been taken into account in order to calculate the cloud condensation nuclei and the corresponding cloud droplet number concentration.

The study shows that cloud radiative properties and indirect forcing are sensitive to cloud microphysical properties such as droplet concentrations and effective radius and macrophysical aspects as the geometrical thickness. Thus, one note the dependence of τ on the both geometrical thickness and the type of clouds.

The investigated influence of cloud geometrical thickness on the cloud albedo and on the indirect forcing shows large different values for various values of the geometrical thickness. That means that dynamical processes in cloud are important in calculating of albedo and radiative forcing.

The albedo increase with the increase of CDNC and decrease when effective radius increase. Therefore, in urban clouds where the droplets are smaller and CDNC larger, the albedo values are larger than in marine clouds.

ACKNOWLEDGEMENTS

This work was sponsored by Romanian CEEX Programme, Contract AMCSIT 112/2005.

REFERENCES

1. Abdul-Razzak, H., Ghan, S.J., and Rivera-Carpio C., *J. Geophys. Res.*, 103, 6123-6132 (1998:);
2. Abdul-Razzak, H., and Ghan, S.J., *J. Geophys. Res.*, 105, 6837-6844 (2000).
3. Boucher, O., Lohmann, U., *Tellus* 47B, 281-300 (1995).
4. Bott, A., *Atmos. Res.*, 53, 15-27 (2000).
5. Charlson R. J., S. E. Schwartz, J. M. Hales, R. D. Cess, J. A. Coakley, JR., J. E. Hansen, and Hofmann, D. J., *Science*, 25, 426-430 (1992.)
6. Conover, J. H., *J. Atmos. Sci.*, 23, 778-785 (1966).
7. Fouquart, Y., Bonnel, B., *Beitr. Phys. Atmos.*, 53 (1980).
8. Ghan, S.J., C.C. Chuang and J. E. Penner, *Atmos. Res.*, 30, 197-221, (1993)
9. Han, Q., Rossow, W. B., Chou, J., Welch, R. M., *J. Climate*, 11 (1998)
10. Hansen, J.E., Travis, L.D., *Space Sci. Rev.*, 16, 527-610 (1974).
11. Hoppe, W.A., and Frick, G.M., *Atmos. Environ.*, 3, 645-659 (1990).
12. Hobbs, P.V., Radke, L. F., and Shumway, S.E., *J. Atmos. Sci.*, 27, 81-89 (1970).
13. Iorga G., S. Stefan, *Roumanian Reports in Physics*, vol 57, No 3, 383-393 (2005).
14. Jaenicke, R., *Aerosol physics and Chemistry*, in Landolt-Boernstein (Ed.), *Zahlenwerte und Funktionen aus Naturwissenschaften und Technik*, Vol. 4b, Springer, 391-457 (1988).
15. Jones, A., D.L. Roberts and A. Slingo, *Nature* 370, 450-453 (1994)
16. Lacis, A.A., Hansen, J.E., *J. Atmos. Sci.*, 31 (1974).
17. Liu, Y., Daum, P.H., *Which size distribution function to use for studies related to effective radius* Proceedings of the 13th International Conference on cloud and precipitation, Reno, NV, 14-18 August;
18. Martin, G.M., Johnson, D.W., Spice, A., *J. Atmos. Sci.*, 51, 13 (1994).
19. Mircea, M., M.C. Facchini, S. Decesari, S. Fuzzi and R. J. Charlson, *Tellus Ser B*, 54B, 74-81, (2002)
20. Pruppacher H. R. and Klett, J.D., *Microphysics of Clouds and Precipitation*, D.Reidel, Dordrecht, 1978, 714pg.
21. Penner, J.E., Charlson, R.J., Hales, J.M. et al. *Bull. Am. Meteorol. Soc.*, 75 (3): 375-400, (1994)
22. Penner, J.E., Dong, X., Chen, Y., *Nature*, 427, 231-234 (2004).
23. Seinfeld J. and S. Pandis, *Atmospheric chemistry an physics*, John Wiley & Sons, 1230pp, 1998
24. Stefan, S., Iorga, G., *Effects of aerosol on the optical properties of clouds*, Proceedings of the 14th International Conference on Clouds and Precipitation, Bologna, Italy, 18-23 July, 2004 pp
25. Twomey, S., *Atmos. Environ.*, 25A, (11), 2435-2442 (1991).
26. Whitby, K.T., *Atmos. Environ.*, 12, 135-159 (1978).
27. **INTERGOVERNMENTAL PANEL ON CLIMATE CHANGE (IPCC), 2001. *Climate Change, The Scientific Basis: Aerosols, their direct and indirect effects*, Intergovernmental Panel on Climate Change, Cambridge University Press, New York.
28. **INTERGOVERNMENTAL PANEL ON CLIMATE CHANGE (IPCC), 1996. *Climate Change 1995, The Science of Climate Change*, J. T. Houghton, L.G. Meira Filho, B. A. Callander, N. Harris, A. Kattenberg, and K. Maskell, (Eds.), Cambridge Univ. Press.